Soft Matter

Accepted Manuscript

ROYAL SOCIETY
OF CHEMISTRY

www.rsc.org/softmatter

Optically Transparent High Temperature Shape Memory Polymer

Xinli Xiao[1,2]*, Xueying Qiu*[1]*, Deyan Kong*[1]*, Wenbo Zhang*[1]*, Yanju Liu*[3]*, Jinsong Leng*[2*]

1. Department of Chemistry, Harbin Institute of Technology, No.92 West Dazhi Street, Harbin 150001, People's Republic of China.

2. Centre for Composite Materials and Structures, Harbin Institute of Technology, No.2 Yikuang Street, Harbin 150080, People's Republic of China.

3. Department of Astronautical Science and Mechanics, Harbin Institute of Technology, No. 92 West Dazhi Street, Harbin 150001, People's Republic of China.

To whom correspondence should be addressed. J. S. Leng (lengjs@hit.edu.cn).

ABSTRACT. Optically transparent shape memory polymers (SMPs) have potentials in advanced optoelectronic and other common shape memory applications, and here optically transparent shape memory polyimide is reported for the first time. The polyimide possess glass transition temperature (T_g) of 171°C, higher than T_g of other transparent SMPs reported, and the influence of molecular structure on T_g is discussed. The 120 μm thick polyimide film exhibits transmittance higher than 81 % in 450-800 nm, and the possible mechanism of its high transparency is analyzed, which will benefit further research on other transparent high temperature SMPs. The transparent polyimide showed nice thermomechanical properties and excellent shape memory performances, and it retained the high optical transparency after many shape memory cycles.

1 Introduction

With the rapid development of optoelectronics, transparent polymers have attracted more and more attention from both academic and engineering applications due to their superior flexibility, lightness and processability compared with the fragile glass analogues.[1-6] Shape memory polymers (SMPs) are smart polymers that can remember the deformed temporary shapes and then recover to the original shape under external stimuli.[7-12] SMPs have been used as biomedical devices,[13-16] smart fabrics,[17] deployable structures,[18] actuators,[19] et al.[20, 21] The optically transparent SMPs possess shape memory effects besides their optical transparency, which will produce some unusual properties. For example, the deformable and adaptive optics made of transparent shape memory poly(ethylene-co-vinyl acetate) (PEVA) can produce real-time optimum device performances, and the phase transition temperature (melting temperature) of PEVA is 63 ºC. [22] Similar to other conventional optically transparent SMPs such as polyester (T_g:~78 ºC) and polystyrene (T_g:~100 ºC), their optical and mechanical properties will be deteriorated at high temperatures.[22-25] Thus the optically transparent polymers with high thermal resistance are greatly desired due to the ever-increasing demands for high reliability and high integration in optoelectronic devices.[3, 5]Accordingly, the optically transparent high temperature SMPs are expected to have potentials in advanced adaptive optoelectronic applications. However, there is no report about highly transparent SMP with T_g higher than 120 ºC until now. [22-28]

Polyimides are high performance polymers due to their high thermal stabilities, excellent mechanical properties and low dielectric constants, and they are good candidates for various fields, including aerospace, automobile, microelectronic and optoelectronic applications.[3,4] The conventional aromatic polyimide films generally possess intense deep colors and poor optical transparency due to the formation of strong intra-/inter-molecular charge transfer complexes

(CTC) interactions, which greatly limits their application in areas where high transparency is the basic need.[1-3] Conversely, the highly transparent polyimide are of special importance for optoelectronic applications such as transparent flexible substrate in displays, flexible printing circuit board, optical waveguides for communication interconnects, and optical half-waveplates for planar lightwave circuits.[4-6] The addition of shape memory effects to the optically transparent polyimide will expand their application enormously. Moreover, the transparent shape memory polyimide is also promising in common shape memory applications that will undergo high temperature environments, such as deployable space structures, jet propulsion systems, high temperature sensors and actuators.[29,30] Although there have been several reports about yellow or brown shape memory polyimides, there is no report about highly transparent shape memory polyimide until now. [31-33]

In the past few decades, many efforts have been made to develop highly transparent low-colored and colorless polyimides by suppressing CTC interactions, such as incorporation of unsymmetrical or bulky pendant units,[34] introduction of strong electron-withdrawing fluorinated or sulfone group,[35] and adoption of alicyclic moieties in the polymer structures.[36] However, most of the above mentioned transparent polyimides demand expensive or intricate reactants.[34-36] In the current report, by employing flexible bis phenol A dianhydride (BPADA) as dianhydride and flexible 1,3-bis(3-aminophenoxy)benzene (BAB) as diamine, as well as controlling the molecular weight, the highly transparent shape memory polyimide are obtained for the first time.

The polyimide exhibits T_g higher than those of other transparent SMPs, and the relationship between molecular structure and T_g is analyzed, and the possible mechanism of its transparency is discussed. The highly transparent polyimide possesses excellent shape memory performances and stable optical properties, which guarantees its potentials in recyclable applications.

2 Experimental

2.1 Synthesis of the transparent shape memory polyimide. BPADA (>98 %) was purchased from TCI and BAB (98 %) were purchased from Sigma-Aldrich Co., and the monomers were used as received. Dimethylacetamide (DMAc) was purchased from Kemiou Chemical Reagent Co. Ltd. and distilled with activated 4 Å molecular sieves under reduced pressure.

4.55 m mol BAB and 20 ml DMAc were added to a three-necked flask and then stirred under dry nitrogen for 20 min. 5 m mol BPADA was fed into the flask in batches within 1 hr, and intense mechanical stirring was executed at room temperature for 22 h to form viscous poly(amic acid) (PAA). The flask was transferred into a vacuum drying chamber and heated under vacuum at 30 ºC for 3 h to remove the bubbles. Thin iron sheets were used as back-up to make sure that the glass substrate is horizontal, as determined by an air-bubble level. The PAA was poured onto the glass substrate and underwent a step-wise imidization curing process at 80 ºC/2 h, 110 ºC /2 h, 160 ºC/2 h, 190 ºC/2 h and 230 ºC/1 h. The polyimide was detached away from glass in deionized water, and heated at 120 ºC for 5 h to remove the water. Other less transparent shape memory polyimide samples with different properties were synthesized with different molar ratio of BPADA to BAB, as shown in the supporting information (Table S1).

2.2 Molecular weight and structure characterization. Molecular weight of polyimide samples were determined by size exclusion chromatography (SEC) using Waters 2414 equipped with a refractive index detector with dimethylformamide (DMF) as eluent at 35 ºC, and the molecular weight versus evolution time was calculated using narrow polydispersity poly(styrene) standards.

The Fourier transform infrared (FT-IR) spectra of the polyimide samples were registered on Thermo Nicolet Nexus 870 from 650 to 4000 cm^{-1} at a resolution of 4 cm^{-1}. X-ray diffraction

(XRD) was carried out on Rigaku Miniflex 600 with Cu Kα radiation (λ=0.15405 nm), and the accelerating voltage and emission current were 40 kV and 50 mA, respectively.

2.3 Optical properties characterization. The ultraviolet-visible (UV-Vis) transmittance of the transparent shape memory polyimide film was executed with Perkin Elmer Lambda 1050 UV/Vis/NIR spectrometer from 200 to 800 nm at a resolution of 1 nm. Three tests were conducted for per sample with each exhibiting the consistent results, and only one transmittance spectra is shown for clarity.

2.4 Thermomechanical and thermal properties characterization. Storage modulus and loss factor of the specimens versus temperature were characterized with dynamic mechanical analysis (DMA) on Netzsch Q800. DMA tests were conducted in tensile mode at the frequency of 1 Hz with a heating rate of 3 ºC/min on slabs with the dimension of 38 mm×3 mm×0.12 mm. The thickness of the slab was the thickness of the film measured, and only the samples with uniform thickness were chosen for DMA analysis. Three tests were conducted for per sample with each exhibiting the consistent results, and only one DMA spectra is shown for clarity.

Differential scanning calorimetric (DSC) were used to characterize the thermal properties of the polymers at a heating rate of 10 ºC /min with NETZSCH STA 449C. The thermal stability of the polyimide was characterized with thermal gravimetric analysis (TGA) under N_2 environment on a Mettler-Toledo TGA/DSC instrument at a heating rate of 10 °C/min.

2.5 Shape memory characterization. The deployable shape memory process of the polyimide was tested with a round sheet. The polyimide sheet was rolled on the surface of hot stage and the deformed shape was fixed by removal from the hot stage to room temperature. Then the sample recovered to its original shape when it was placed back to the hot stage, and the shape recovery process was recorded with a digital video (Canon VIXIA HF R500).

The stretchable shape memory performance was executed with consecutive stretch-contraction processes using the controlled force mode on TA INSTUMENT Q800. The steps are carried out as follows: (a) heating a sample to T_g+20 °C, (b) applying a force that would prolong the sample; (c) reducing to T_g-40 °C, (d) force removal, (e) heating to T_g+20 °C. Once the sample recovered to a constant value, the process was repeated by applying the same force used in step (b).

3 Results and Discussions

3.1 Molecular weight and structures. The polycondensation process of the highly transparent shape memory polyimide (TSMPI) is shown in Scheme 1. The highly TSMPI possesses number average molecular weight (M_n) of 21.7 kg/mol and weight average molecular weight (M_w) of 42.5 kg/mol. The polyimide samples with higher M_n are less transparent than the almost colorless polyimide, while the samples with lower M_n don't possess shape memory effects, as summarized in the supporting information (Table S1).

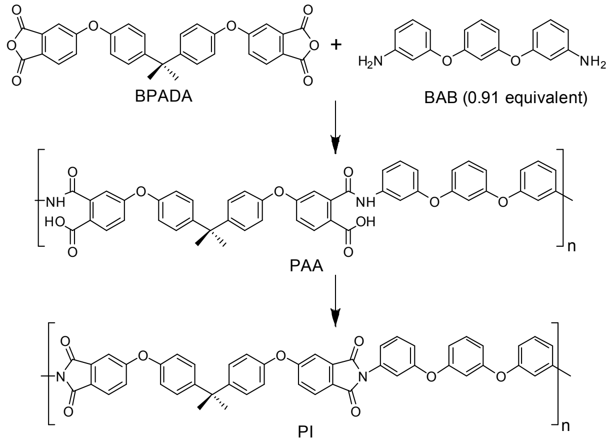

Scheme 1. Polycondensation of the highly transparent shape memory polyimide

The representative section of IR spectra (800-2000 cm^{-1}) of TSMPI are shown in Figure 1a, and the peaks around 1780 cm^{-1} (asymmetric stretching of C=O), 1718 cm^{-1} (symmetric stretching of C=O) and 1373 cm^{-1} (stretching vibration of C-N-C) confirm the formation of imides. There is no evidence of carbonyl peaks of isoimide in 1795-1820 or 921-934 cm^{-1}, indicating the absence of isoimides. The carbonyl stretching in an inter-molecular imide linkage near 1670 cm^{-1} is not observed, either.[38] These results demonstrate that the sample is fully imidized within the detection limit of IR. The typical IR peaks of PAA disappeared and the characteristic peaks of polyimide appeared after thermal curing, as manifested in the supporting information (Figure S1), and the IR spectra of other less transparent shape memory polyimides are shown in the supporting information (Figure S2).

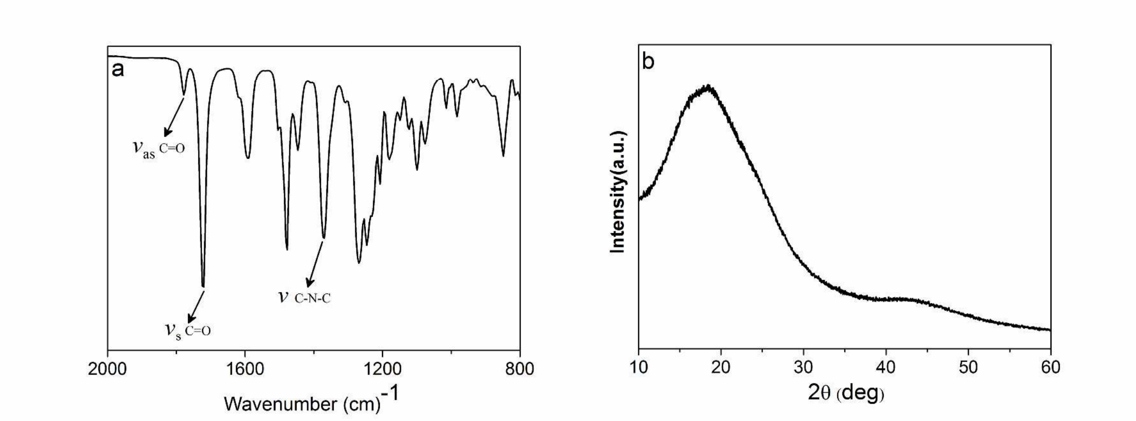

Figure 1. FT-IR(a) and XRD (b) spectra of TSMPI.

The wide-angle X-ray diffraction pattern of TSMPI is shown in Figure 1b, and it displays broad peak centered at about 18 ° due to the diffraction of intermolecular packing, characteristic of some regularity combined with amorphous halo.[34] The XRD results manifest that the polyimide are amorphous in morphologic structures, mainly due to the loose chain packaging and aggregation caused by the ether and isopropylidene linkages in dianhydride, as well as the meta-substituted ether linkages in the diamine units. The XRD spectra of other less transparent polyimide samples are shown in the supporting information (Figure S3).

3.2 Optical transparency. The optical properties of the polyimide was evaluated by both UV-Vis spectra and their physical appearance. As illustrated in Figure 2, the 120 μm thick TSMPI film shows very good optical transparency, its cut-off wavelength value (λ_0) is 381 nm, and the transmittance at 450 and 500 nm is 82 % and 85 %, respectively. Optical photographs of the TSMPI film is shown in the inlet, and it is observed that the highly transparent TSMPI is almost colorless. The thickness of the film can affect its optical property, and UV-Vis spectra of the TSMPI film with different thickness are shown in the supporting information (Figure S4). Thicker film will lead to less transparency, and the transmittance at 450 nm for films with thickness of 120, 180, 260 and 320 μm is 82 %, 79 %, 75 % and 71 %, respectively. The UV-Vis spectra of other less transparent shape memory polyimide samples are shown in the supporting information (Figure S5), and their cut-off wavelength values and transmittance are summarized in the supporting information (Table S2).

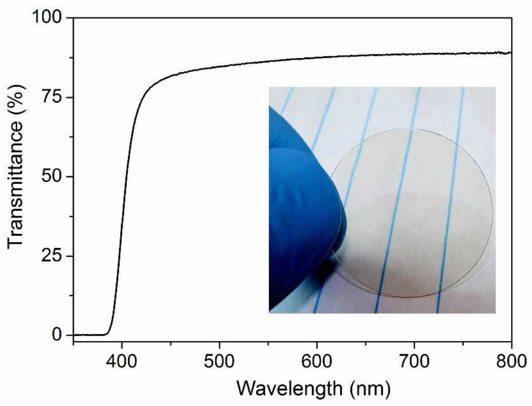

Figure 2. UV-Vis spectra of 120 μm thick TSMPI film, and inlet shows its optical photograph.

It has been proved that the coloration of aromatic PIs is mainly caused by the intra-/inter-molecular charge transfer complex (CTC) formation between the alternating electron-acceptor (dianhydride) and electron-donor (diamine) moieties, and higher CTC interactions lead to deeper colors.[1,3,5] In this regard, the high transparency of TSMPI originates from the strongly suppressed CTC interactions, and the 3-dimensional (3D) molecular structure of TSMPI is shown in Figure 3.

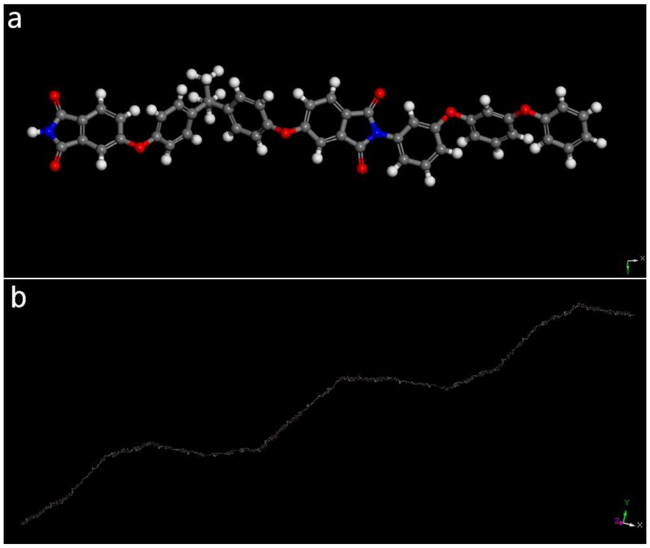

Figure 3. Three-dimensional structures of structural unit (a) and polyimide chain (b) of TSMPI. The grey, white, red and blue of molecular structure display C, H, O and N, respectively.

As can be observed from Figure 3a, the introduction of large pendant isopropyl groups in the dianhydride will increase the free volume of each molecule and destroy the compact stacking of molecular chains, thus decreasing the intermolecular CTC interactions. The isopropyl groups and the flexible ether linkage in the dianhydride can hinder the charge flow along the main chains, which will suppress the intramolecular CTC interactions. The molecular structure is folded when meta-substituted, and the intermolecular CTC interactions decreased. Both the meta-substituted structures and flexible ether linkage in the diamine can decrease charge flow, which will reduce the intramolecular CTC interactions. Consequently, the formation of both inter- and intra-molecular CTC interactions are obstructed. It is well-known that the intermolecular interactions of polymers will become weaker for samples with lower M_n, thus colors of the polyimide samples get lower and lower with the decrease of M_n and TSMPI becomes almost colorless, as shown in the supporting information (Figure S6). Judged from M_n (21.7 kg/mol) and structural unit (807g/mol), a typical TSMPI molecular chain comprises 27 structural units, and its characteristic folded 3D molecular structure is shown in Figure 3b. But the polyimide samples with M_n lower that of TSMPI can't produce good shape memory effects, indicating that chain entanglements are essential for shape memory process of thermoplastic polyimide.[12, 30, 31] The folded long chains are apt to form chain entanglements, and the molecular chains of samples with lower M_n are less folded, as illustrated by their 3D structures in the supporting information (Figure S7).

The development of transparent PI has been affected by the high cost of commercial available monomers negatively, as the cost of transparent PI films is largely determined by the monomers.[39] Most of the reported highly transparent polyimide samples are synthesized with intricate and expensive reagents, and some typical monomers for transparent PIs, such as 1,2,3,4-cyclobutane tetracarboxylic dianhydride (5 g/1850 CNY),[40, 41] 3,4-dicarboxy-1,2,3,4-tetrahydro-1-naphthalene succinic dianhydride (5 g/690 CNY),[37, 40] and 2,2'-bis(3,4-dicarboxyphenyl) hexafluoro-propane dianhydride (5 g/1990 CNY) are rather expensive. [40, 42] Compared with them, the 2,2-bis[4-(3,4-dicarboxyphenoxy)phenyl]propane dianhydride (25 g/790 CNY) used in this report is relatively cheap. Some other monomers for transparent PIs such as 9,9-bis[4-(4-amino-2-trifluoromethylphenoxy) phenyl] fluorene,[39] 1,4-bis[4-amino-2-trifluoromethylphenoxy]-2,5-di-tertbutylbenzene,[43] and 2,2'-bis[4-(3-nitro-5-trifluoromethylphenoxy)phenyl] sulfone are synthesized in the authors' own lab with intricate ways,[34] and they are not commercially available. Here we offered an economical way to obtain optically transparent polyimide with common reactants.[40] TSMPI can be dissolved in DMF, DMAc and NMP, and the solubility can be explored to produce films at low temperature, avoiding the possible damages to optoelectronic devices caused by high temperature. [4,34]

3.3 Thermomechanical and thermal properties. The thermomechanical properties of TSMPI are analyzed with DMA, as shown in Figure 4. It is observed that the tensile storage modulus (*E'*) decreases slowly with the increase of temperatures in glassy state, but there is an essential decrease around T_g, and the storage modulus of TSMPI at 50 ºC, 151 ºC (T_g-20 ºC) and 191 ºC (T_g+20 ºC) are 2.2 GPa, 1.7 GPa and 4.1 MPa, respectively.

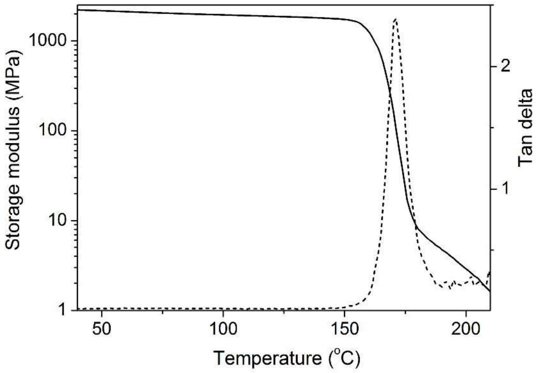

Figure 4. Tensile storage modulus (solid line)and loss factor (dotted line) versus temperature of the TSMPI.

The peak of loss factor (tan δ) obtained by DMA is often taken as T_g of rigid-chain polymers, and TSMPI exhibits T_g of 171 ºC, which is higher than those of other transparent SMPs, but lower than those of shape memory polyimides. It has been proved that the relative flexibility of the polymer backbone can affect dynamics through the glass transition,[39 44] which has great influence on T_g of polymers. Many SMPs composed of polymers with flexible main chains possess T_g lower than 110 ºC, while high temperature SMPs, such as polyimide, polycayanate and poly(ether ether ketone) ionomers, are composed of rigid main chains comprising phenyl rings and flexible linkages.[8, 32, 37] Shape memory polyimides are obtained from polycondensation of dianhydride and diamine, and the TSMPI in this report is obtained from BAB and BPADA. The isopropylidene and ether linkages within the backbone, together with the meta-substitute structure provide flexibility to the rigid polyimide molecule, and the molecular chains act as reversible phase of the shape memory process. The shape memory polyimide samples obtained from polycondensation of BPADA/2,2-bis[4-4(-aminophenoxy) phenyl] propane (BAPP), 4,4'-(hexafluoroisopropylidene) diphthalic anhydride (6FDA)/BAB and 4,4′-oxydiphthalic dianhydride (ODPA)/4,4'-diaminodiphenyl ether (ODA) exhibited T_g of 212 °C, 222 °C and 261 ºC, respectively.[31, 32, 45] The molecular structures of the typical shape memory polyimide samples are illustrated in the supporting information (Figure S8). For the dianhydrides of shape memory polyimides, BPADA possesses one isopropylidene and two ether linkages, 6FDA possesses one hexafluoroisopropylidene, and ODPA possess one ether linkage in the backbone. Among them, BPADA is the most flexible dianhydride. For the diamines, BAPP possesses an isopropylidene and two ether linkages in the highly symmetrical manner, BAB possesses two meta-substituted ether linkages, and ODA possesses one ether linkage in the backbone. Among them, BAB is the most flexible diamine. From the standpoint of molecular structures, it is obvious that the main-chain flexibility of the different types of shape memory polyimide samples are arranged in the sequence of BPADA/BAB>BPADA/BAPP>6FDA/BAB>ODPA/ODA. As a result, the polyimide of BPADA/BAB exhibits T_g lower than those of the previously reported shape memory polyimides. The modulus and tan δ of other less transparent shape memory polyimides are shown in the supporting information (Figure S9).

The thermal stability of the TSMPI is examined with TGA, and the weight loss and derivative of weight are shown in Figure 5. The major decomposition was observed by examining the derivative of the weight curves, and the sample shows high thermal stability with minimal decompositions (<5%) to 485 ºC before major decompositions beginning at 540 ºC. The pyrolysis left about 46 % carbonaceous char at 800 °C, and these results indicate that TSMPI are thermally stable. The TGA spectra of other less transparent shape memory polyimide samples are shown in the supporting information (Figure S10).

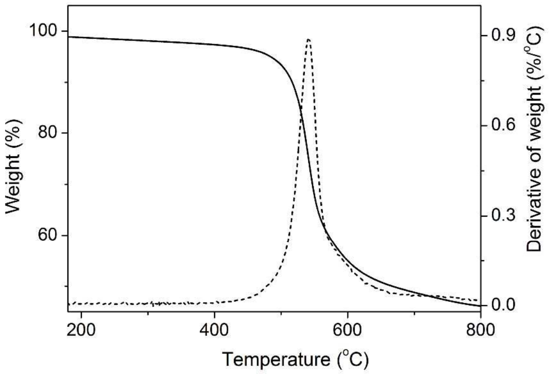

Figure 5. TGA spectra of the weight loss (solid line) and derivative of weight (dashed line) of TSMPI.

3.4 Shape memory properties. Deployable application is the commonly used pattern of SMP, and the shape memory properties are studied with a round polyimide sheet. The sheet was rolled on a hot stage, and the–temporary shape was fixed by cooling to room temperature. Then the sample recovered to its original shape when it was placed back to the same hot-stage. The typical images showing the deformed shape and the consequent shape recovery process of SMTPI5 are shown in Figure 6, and the movie is in the supporting information (Movie S1). The process is repeated thirty times with no damage observed, and every time it appears to recover completely to the initial shape.

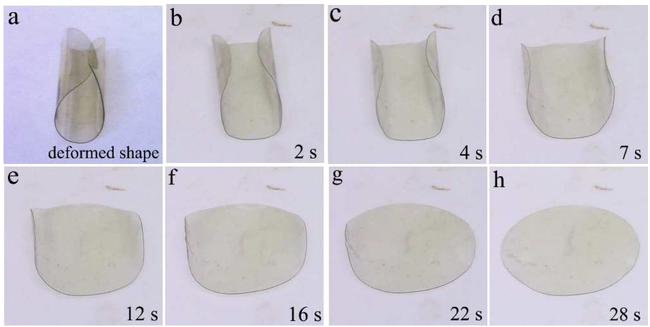

Figure 6. Deployable shape memory pattern of TSMPI. (a) deformed temporary shape and (b)-(h) shape recovery process of TSMPI on 190 ºC hot-stage, and the subscripts indicate the time on the hot-stage.

Stretchable application is another commonly used pattern, and it is also usually employed to determine shape recovery (R_r) and shape fixity (R_f) of SMPs. R_r and R_f are two important factors in determining shape memory performances of SMP, which represents the capability of the SMP to recover to its original shape and maintain the mechanical deformation, respectively. R_r is calculated with Equation 1.

$$R_r(N) = \frac{\varepsilon_m(N)-\varepsilon_p(N)}{\varepsilon_m(N)-\varepsilon_p(N-1)} \times 100\ \% \qquad (1)$$

ε_m, ε_p and N denote the strain after the stretching step (before cooling), the strain after recovery, and the cycle number, respectively. R_f is calculated using Equation 2.

$$R_f(N) = \frac{\varepsilon_u(N)}{\varepsilon_m(N)} \times 100\ \% \qquad (2)$$

ε_u denote the strain in the fixed temporary shape. The stretchable pattern was examined with consecutive stretch-contraction cycles, and the cycles of TSMPI are shown in Figure 7.

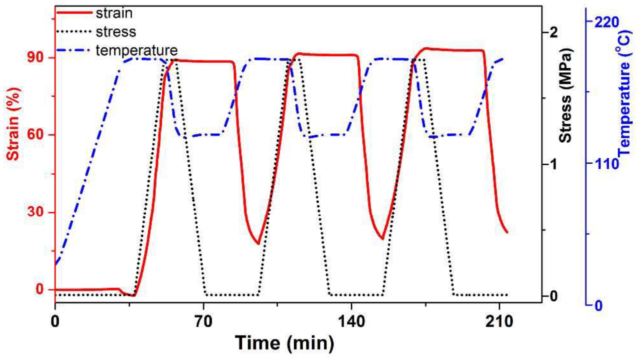

Figure 7. The stretchable shape memory process of TSMPI with two-dimensional demonstration of changes in strain, stress and temperature versus time.

It is observed that R_f of the first, second and third cycle is 99.2 %, 99.3 % and 99.2 %, respectively, consistent from one cycle to another. However, R_r is 80.1 % for the first cycle, 97.6 % and 97.0 % for the second and third cycle. The difference in R_r between the first and the following cycles is generally ascribed to the residual strain resulting from the processing history.[46]TSMPI possesses excellent shape memory properties, mainly due to the large difference in storage modulus at glassy and rubbery states. [8, 47] The high storage modulus in glassy state originates from the potential elasticity, and the low storage modulus in rubbery state is caused by the entropy elasticity due to the micro-Brownian movement.

3.5 Optical stability. Stable optical properties of TSMPI are of great importance for their applications, as they may be exposed not only to disposable but also to recyclable devices. Here the optical stability is characterized with transmittance of the sample after 5, 10, 15, 20 and 30 shape memory cycles, as shown in Figure 8.

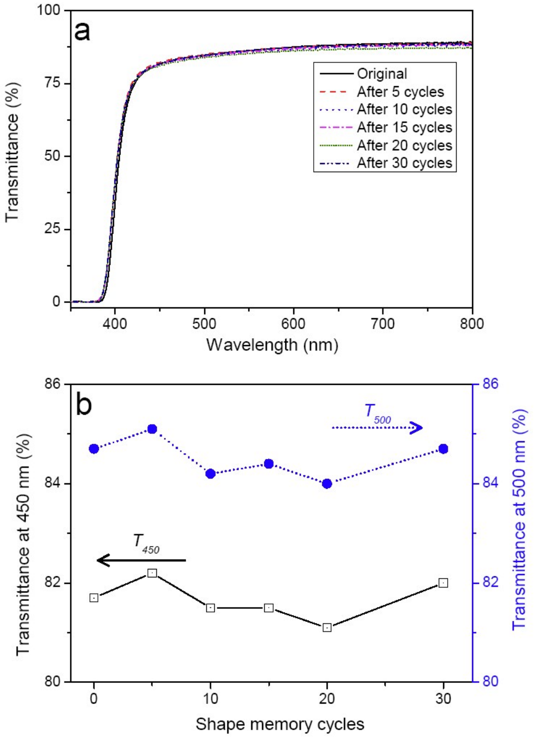

Figure 8. Optical properties of TSMPI exposed to shape memory cycles. (a) Transmittance before and after 5, 10, 15, 20 and 30 shape memory cycles at 350-800 nm. (b) Particular transmittance values at 450 and 500 nm after different cycles.

It is observed that there is almost no discernable difference in transmittance from Figure 8a. The particular transmittance values at 450 and 500 nm are shown in Figure 8b, and there is no trend of degradation within the characterized shape memory cycles. These results indicate that TSMPI possesses stable optical properties, which will benefit their applications as recyclable optoelectronic devices.

4 Conclusion

In summary, this report has offered an efficient way to obtain optically transparent shape memory polyimide that have vast potentials by controlling chemical structure and molecular weight. The high optical transparency mainly originates from the suppressed intra-/inter molecular charge transfer complex interactions caused by the special structure of the polyimide. The transparent shape memory polyimide shows T_g of 171 ºC, higher than those of other optically transparent SMPs. The transparent polyimide exhibits excellent shape memory properties, and it retains the stable optical transparency after shape memory cycles. The combination of unusual optical properties with shape memory effects guarantee its foreseeable applications in advanced optoelectronic devices and other high temperature applications

Acknowledgements

This research is financially supported by National Natural Science Foundation of China (Granted No.51402073, 11225211 and 11272106), China Postdoctoral Science Foundation (Granted No.2013M531030), and Fundamental Research Funds for the Central Universities (Grant No. HIT. NSRIF. 2011018 and HIT. NSRIF. 2012064).

Electronic Supplementary Information (ESI) available: Molecular weight, IR, XRD, optical photograph, UV-Vis transmittance, DMA, TGA of other less transparent shape memory polyimides, IR spectra of poly(amic acid) (PAA), UV-Vis transmittance of TSMPI films with different thickness, three-dimensional structures of the polyimide chains with different molecular weight, molecular structures of reported shape memory polyimides, and the video showing deployable shape recovery process of TSMPI are shown in ESI.

Notes

The authors declare no competing financial interests.

References

(1) K. Mizoguchi, Y. Shibasaki and M. Ueda, *J. Photopolym. Sci. Technol.,* 2007**, 20,** 181-186.

(2) J. M. Liu, T. M. Lee, C. H. Wen and C. M. Leu, *J. Soc. Inf. Display,* 2011, **19,** 63-69.

(3) M. C. Choi, J. C. Hwang, C. Kim, S. Ando and C. S. Ha, *J. Polym. Sci. Part A Polym Chem,* 2010**, 48,** 1806-1814.

(4) K. Takizawa, J. Wakita, S. Azami and S. Ando, *Macromolecules,* 2011**, 44***,* 349-359.

(5) C. P. Yang and Y. Y. Su, *Polymer,* 2005, **46,** 5797-5807.

(6) J. C. Kim and J. H. Chang, *Macromol. Res.,* 2014, **22,** 1178-1182.

(7) G. Tandon, K. Goecke, K. Cable and J. *J.* Baur, *Int. Mater. Syst. Struct.,* 2009, **20,** 2127–2143.

(8) I. A. Rousseau, *Polym. Eng. Sci.,* 2008, **48,** 2075–2089.

(9) F. Pilate, R. Mincheva, J. D. Winter, P. Gerbaux, L. Wu, R. Todd, J. M. Raquez and P. Dubois, *Chem. Mater.*, 2014, **26,** 5860–5867.

(10) X. D. Jin, Q. Q. Ni and T. Natsuki, *J. Comp. Mat.,* 2011**, 45,** 2547-2554.

(11) M. Behl, M. Y. Razzaq and A. Lendlein, *Adv. Mater.,* 2010, **22,** 3388–3410.

(12) X. L. Xiao, D.Y. Kong, X. Y. Qiu, W. B. Zhang, Y. J. Liu, S. Zhang, F. H. Zhang, Y. Hu and J. S. Leng, *Sci. Rep.,* 2015, **5,** 14137.

(13) K. Yu, Q. Ge and H. J. Qi, *Nat. Comm.,* 2014, **5,** 3066.

(14) C. M. Yakacki, R. Shandas, C. Lanning, B. Rech, A. Eckstein and K. Gall, *Biomaterials,* 2007**, 28,** 2255–2263.

(15) K. Nagahama, Y. Ueda, T. Ouchi and Y. Ohya, *Biomacromolecules,* 2009**, 10,** 1789−1794.

(16) H. Chen, Y. Li, Y. Liu, T. Gong, L. Wang and S. Zhou, *Polym. Chem.*, 2014, **5,** 5168–5174.

(17) J. Hu, Y. Zhu, H. Huang and J. Lu, *Prog. Polym. Sci.,* 2012**, 37,** 1720–1763.

(18) W. M. Sokolowski and S. C. Tan, *J. Spacecraft & Rockets,* 2007, **44,** 750–754 .

(19) Y. P. Liu, K. Gall, M. L. Dunn, A. R. Greenberg and J. Diani, *Int. J. Plast.,* 2006, **22,** 279–313.

(20) K. Kratz, S. A. Madbouly, W. Wagermaier and A. Lendlein, *Adv. Mater.,* 2011**, 23,** 4058–4062.

(21) Y. Y. Zhang, Y. M. Li and W. G. Liu, *Adv. Func. Mater.,* 2015**, 25,** 471–480.

(22) H. X. Xu, C. J. Yu, S. D. Wang, V. Malyarchuk, T. Xie and J. A. Rogers, *Adv. Funct. Mater.,* 2013, **23,** 3299–3306.

(23) C. S. Zhang, Q. Q. Ni, S. Y. Fu and K. Kurashiki, *Comp. Sci. and Tech*., 2007, **67,** 2973–2980.

(24) H. G. Jeon, P. T. Mather and T. S. Haddad, *Polym. Int.,* 2000, **49,** 453–457.

(25) T. F. Scott, R. B. Draughon and C. N. Bowman, *Adv. Mater.,* 2006, **18,** 2128–2132.

(26) J. M. Haberl, A. Sánchez-Ferrer, A. M. Mihut, H. Dietsch, A. M. Hirt and R. Mezzenga, *Adv. Funct. Mater.,* 2014, **24,** 3179–3186.

(27) J. J. Song, H. H. Chang and H. E. Naguib, *Polymer.,* 2015**, 56,** 82-92.

(28) A. Khaldi, J. A. Elliott and S. K. Smoukov, *J. Mater. Chem. C.,* 2014**, 2**, 8029–8034.

(29) Y. Shi and R. A. Weiss, *Macromolecules,* 2014, **47,** 1732−1740.

(30) X. L. Xiao, D.Y. Kong, X. Y. Qiu, W. B. Zhang, F. H. Zhang, L. W. Liu, Y. J. Liu, S. Zhang, Y. Hu and J. S. Leng, *Macromolecules,* 2015, **48,** 3582-3589.

(31) M. Yoonessi, Y. Shi, D. A. Scheiman, M. Lebron-Colon, D. M. Tigelaar, R. A. Weiss and M. A. Meador, *Acs Nano,* 2012, **6,** 7644–7655.

(32) H. Koerner, R. J. Strong, M. L. Smith, D. H. Wang, L. S. Tan, K. M. Lee, T. J. White and R. A. Vaia, *Polymer,* 2013, **54,** 391–402.

(33) J. A. Shumaker, A. J. W. McClung and J. W. Baur, *Polymer,* 2012, **53,** 4637–4642.

(34) L. Zhai, S. Y. Yang and L. Fan, *Polymer,* 2012, **53,** 3529-3539.

(35) Y. M. Kim and J. H. Chang, *Macromolecular Res.,* 2013**, 21,** 228-233.

(36) H. Masatoshi, F. Mari, I. Junichi, Y. Shinya, T. Eiichiro, K. Takashi and I. Atsushi, *Polymer,* 2014, **55,** 4693-4708.

(37) H. J. Ni, J. G. Liu, Z. H. Wang and S. Y. Yang, *J. Ind. Eng. Chem.*, 2015, **28**, 16–27.

(38) C. A. Pryde, *J. Polym. Sci. Part A. Poly. Chem.,* 1989, **27,** 711–724.

(39) C. P. Yang, Y. Y. Su and Y. C. Chen, *Eur. Polym. J.* 2006, **42**, 721–732.

(40) Websites of Tokyo Chemical Industry. http://www.tcichemicals.com/zh/cn/product/index.html.

(41) H. Suzuki, T. Abe, K. Takaishi, M. Narita and F. Hamada, *J. Polym. Sci., A: Polym. Chem.* 2000, **38**, 108-116.

(42) T. L. Li and S. L. C. Hsu, *Eur. Polym. J.* 2007, **43**, 3368-3373.

(43) C. P. Yang and F. Z. Hsiao, *J Polym Sci Part A: Polym Chem* 2004, **41**, 2272-227.

(44) J. D. Merline, N. C. P. Reghunadhan, C. Gouri, G. G. Bandyopadhyay and K. N. Ninan, *J. Appl. Polym. Sci*., 2008, **107,** 4082–4092.

(45) Q. H. Wang, Y. K. Bai, Y. Chen, J. P. Ju, F. Zheng and T. M. Wang, *J. Mater. Chem. A*, 2015, **3**, 352-359.

(46) T. Xie and I. A. Rousseau, *Polymer*, 2009, **50,** 1852–1856.

(47) K. Yu, T. Xie, J. S. Leng, Y. F. Ding and H. J. Qi, *Soft Matter* 2012, **8,** 5687–5695.

Optically Transparent High Temperature Shape Memory Polymer

Xinli Xiao, Xueying Qiu, Deyan Kong, Wenbo Zhang, Yanju Liu, Jinsong Leng[*]

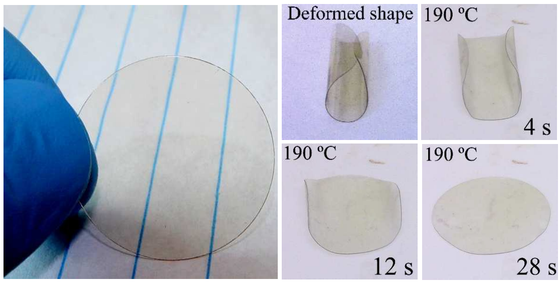

Optically transparent shape memory polyimide exhibiting glass transition temperature higher than those of other transparent shape memory polymers is reported.